ADVANCES IN ATMOSPHERIC SCIENCES, VOL. 39, JULY 2022, 1198–1206

• **Letters and Notes** •

The Warming of the Tibetan Plateau in Response to Transient and Stabilized 2.0°C/1.5°C Global Warming Targets※

Jintao ZHANG[1,2], Qinglong YOU[*1,3,4], Fangying WU[1], Ziyi CAI[1], and Nick PEPIN[5]

[1]*Institute of Atmospheric and Oceanic Sciences*, *Fudan University*, *Shanghai* 200438, *China*

[2]*Chinese Academy of Meteorological Sciences*, *China Meteorological Administration*, *Beijing* 100081, *China*

[3]*Innovation Center of Ocean and Atmosphere System*, *Zhuhai Fudan Innovation Research Institute*, *Zhuhai* 518057, *China*

[4]*CMA-FDU Joint Laboratory of Marine Meteorology*, *Shanghai* 200438, *China*

[5]*School of Environment*, *Geography, and Geosciences*, *University of Portsmouth*, *Portsmouth PO*1 3*HE*, *U.K*

(Received 31 July 2021; revised 19 March 2022; accepted 22 March 2022)

ABSTRACT

As "the third pole", the Tibetan Plateau (TP) is sensitive to climate forcing and has experienced rapid warming in recent decades. This study analyzes annual and seasonal near-surface air temperature changes on the TP in response to transient and stabilized 2.0°C/1.5°C global warming targets based on simulations of the Community Earth System Model (CESM). Elevation-dependent warming (EDW) with faster warming at higher elevations is predicted. A surface energy budget analysis is adopted to uncover the mechanisms responsible for the temperature changes. Our results indicate a clear amplified warming on the TP with positive EDW in 2.0°C/1.5°C warmer futures, especially in the cold season. Mean TP warming relative to the reference period (1961–90) is dominated by an enhanced downward longwave radiation flux, while the variations in surface albedo shape the detailed pattern of EDW. For the same global warming level, the temperature changes under transient scenarios are ~0.2°C higher than those under stabilized scenarios, and the characteristics of EDW are broadly similar for both scenarios. These differences can be primarily attributed to the combined effects of differential downward longwave radiation, cloud radiative forcing, and surface sensible and latent heat fluxes. These findings contribute to a more detailed understanding of regional climate on the TP in response to the long-term climate goals of the Paris Agreement and highlight the differences between transient and stabilized warming scenarios.

Key words: elevation-dependent warming (EDW), Paris Agreement, Tibetan Plateau, transient and stabilized warming, temperature

Citation: Zhang, J. T., Q. L.You, F. Y. Wu, Z. Y. Cai, and N. Pepin, 2022: The warming of the Tibetan Plateau in response to transient and stabilized 2.0°C/1.5°C global warming targets. *Adv. Atmos. Sci.*, **39**(7), 1198–1206, https://doi.org/10.1007/s00376-022-1299-8.

Article Highlights:

- Future TP warming relative to the present-day is strongly correlated with changes in downward clear-sky longwave radiation.
- Elevation-dependent warming with higher rates of warming at higher elevations results from uneven changes in surface albedo.
- TP warming is ~0.2°C higher under transient scenarios than for stabilized scenarios at the same global warming target.

1. Introduction

The Tibetan Plateau (TP), with an area of 2.5 × 10^6 km^2 and an average elevation of over 4000 m above sea level, is the highest and most extensive plateau in the world. The TP is known as "the third pole" of the Earth and the "Water Tower of Asia" (Kang et al., 2010; Yao et al., 2012). The near-surface temperature has significantly increased on the TP, and this trend is projected to continue in future scenarios (You et al., 2016, 2021). Along with mountain ranges around the world, the rapid warming on the TP and its impacts on the cryosphere, ecology, hydrology, etc. have been of intense interest in recent Earth system sciences (Duan et al., 2012; Zhang et al., 2018; Yao et al., 2019; You et al., 2020a; Wang et al., 2021).

※ This paper is a contribution to the special issue on Third Pole Atmospheric Physics, Chemistry, and Hydrology.

* Corresponding author: Qinglong YOU
Email: qlyou@fudan.edu.cn

The Paris Agreement, which aims to address climate change, has attracted much attention worldwide (UNFCCC, 2015). Recently, much effort has been made to investigate regional temperature changes under the Paris Agreement temperature targets. These are to limit global warming below 2.0°C above pre-industrial levels and pursue efforts to limit it to 1.5°C (e.g., Zhang and Wang, 2019; Shi et al., 2020). Many previous studies have shown amplification of future temperature changes over the TP relative to surrounding areas and globally averaged warming (You et al., 2020a, 2021). The additional 0.5°C of global warming (between 1.5°C and 2.0°C) is projected to lead to a significant additional increase in temperature on the TP (Fu et al., 2018; Wu et al., 2019; Shi et al., 2020). However, most of the above studies are based on transient global climate model simulations as they pass through the 2.0°C/1.5°C threshold, and these may not be consistent with stabilized 2.0°C/1.5°C climate states. The potential difference in changes in regional temperature on the TP in stabilized versus transient simulations has not been examined. In addition, many previous studies have reported elevation-dependent warming (EDW) on the TP (Cai et al., 2017; You et al., 2019; Li et al., 2020; Niu et al., 2021). However, any differences in EDW on the TP under transient versus stabilized 2.0°C/1.5°C global warming scenarios are unclear.

Therefore, this study analyzes both the annual and seasonal changes near-surface temperature on the TP in response to transient and stabilized 2.0°C /1.5°C global warming targets. We perform our simulations using the Community Earth System Model (CESM). Temperature changes and their physical mechanisms in different elevation ranges were examined. Our results contribute to a more detailed understanding of climate and environmental change on the TP in response to global climate forcing and will provide further details for climate change adaptation on the ecologically fragile TP.

The remainder of this paper is organized as follows. Section 2 describes the data and methods used in this study. Section 3 presents the projected changes in near-surface air temperature on the TP under transient and stabilized 2.0°C/1.5°C global warming scenarios, and further examines influence factors of temperature change from the perspective of surface energy budget analysis. Section 4 provides a discussion and conclusion.

2. Data and methods

Previous studies have suggested that CESM can reasonably reproduce the historical climatology and trend of mean near-surface air temperature on the TP (You et al., 2016; Lun et al., 2021), which provides credible evidence that CESM can be adopted for future climate projections. Monthly outputs of the historical simulation (1850–2005) and future projections (2006–2100) for two Representative Concentration Pathway (RCP) scenarios (i.e., RCP8.5 and RCP4.5, Kay et al., 2015; Sanderson et al., 2018) and low-warming scenarios (Sanderson et al., 2017) were obtained from the CESM experiments data archive (Table 1). Due to data availability limitations, the RCP4.5 simulation only lasts until 2080. We only used the first 11 members of all CESM simulations for consistency among scenarios. The topography of the TP used in CESM is displayed in Fig. 1.

In the following analysis, the transient climate response is derived from both RCP8.5 and RCP4.5. The timings of the 2.0°C and 1.5°C warming above pre-industrial (1850–1920) levels are determined using the 11-year running mean of the global mean near-surface air temperature calculated from the ensemble mean (Table 1, Fig. 2). The stabilized climate response is derived from low-warming simulations of CESM in which the global mean temperature reaches ~2.0°C/1.5°C by the end of the 21st century (Table 1, Fig. 2).

The Coupled Model Inter Comparison Project phase 6 (CMIP6), which includes various coupled general circulation models, is now available (Tebaldi et al., 2021). Although CESM is not the latest model compared to CMIP6, its low-warming simulations provide a rather complete description of the climate system at stabilized levels, which is not available in CMIP-type simulations. Note that "stabilized" in this study means a short-term stabilization response (late 21st-century output of simulations driven with emissions that stabilize mean global warming to 1.5°C/2.0°C by 2100), which is different from "equilibrium" or "control" simulations (where external radiative forcings are fixed) (Sanderson et al., 2017).

The surface energy budget equation proposed by Lu

Table 1. Time periods during which global warming reaches 2.0°C/1.5°C relative to pre-industrial temperatures under different scenarios and their corresponding radiative forcing.

Global warming		Ensemble members	1.5°C–ref		2.0°C–ref		2.0°C–1.5°C
			Time period	Radiative forcing (W m^{-2})	Time period	Radiative forcing (W m^{-2})	Radiative forcing (W m^{-2})
Transient scenarios	RCP8.5	40*	2023–33	~3.0	2035–45	~3.7	~0.7
	RCP4.5	15*	2031–41	~3.1	2050–60	~3.6	~0.5
Stabilized scenarios	Low-warming 2.0°C	11			2090–2100	~3.2	~1.0
	Low-warming 1.5°C	11	2090–2100	~2.2			

* Only the first 11 members of each simulation were adopted for consistency among scenarios.

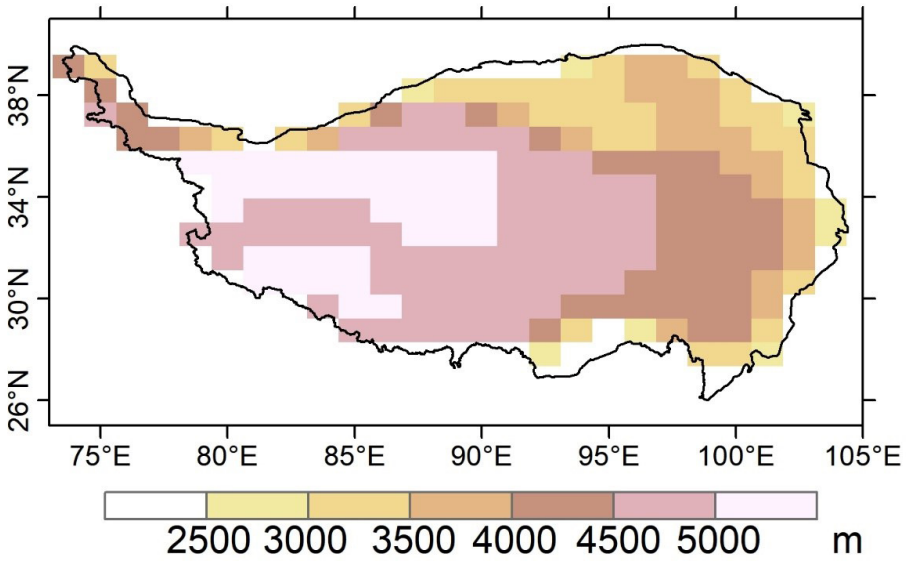

Fig. 1. Topography of the Tibetan Plateau as represented in the CESM model. The elevation of the highest grid point in CESM is 5280 m.

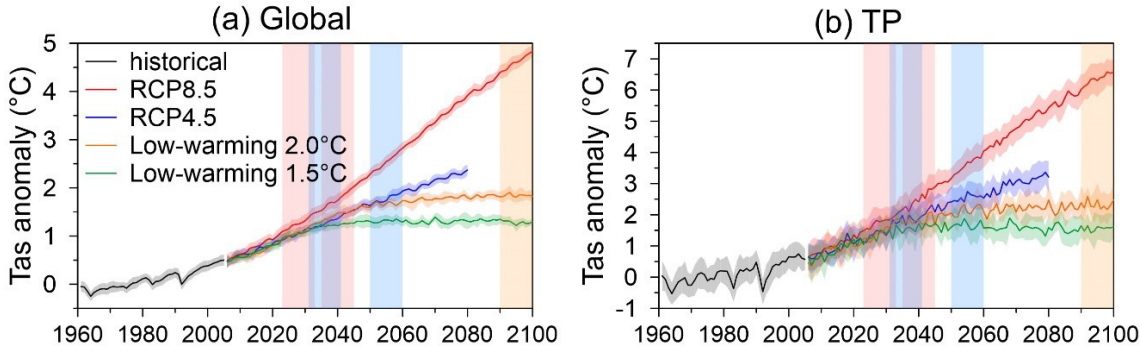

Fig. 2. Time series of (a) global and (b) Tibetan Plateau averaged annual mean near-surface air temperature anomaly (relative to pre-industrial levels) in CESM simulations. Vertical color bars in red, blue, and orange indicate the time period in which global warming reaches the 2.0°C/1.5°C threshold in RCP8.5, RCP4.5, and low-warming simulations, respectively (see Table 1).

and Cai (2009) is adopted to explain the mechanisms of temperature changes on the TP. The surface temperature change (ΔTs) can be decomposed into seven terms (Eq. 1), including surface albedo feedback (SAF), changes in cloud radiative forcing (CRF), the non-SAF-induced change in clear-sky shortwave (SW) radiation, the change in downward clear-sky longwave (LW) radiation, the change in heat storage, combined changes in surface sensible/latent heat fluxes, and the residual of this decomposition (usually very small).

$$4\sigma\overline{T}_s^3\Delta T_s = (-\Delta\alpha)\left(\overline{\mathrm{SW}}^{\downarrow} + \Delta\mathrm{SW}^{\downarrow}\right) + \Delta\mathrm{CRF} + (1-\overline{\alpha})\Delta\mathrm{SW}^{\downarrow}_{\mathrm{clr}} + \Delta\mathrm{LW}^{\downarrow}_{\mathrm{clr}} + (-\Delta Q) + [-\Delta(H+LE)] + \delta\,. \quad (1)$$

Here the overbar indicates the climatology for the reference period, and Δ means the difference between the climatologies of future scenarios and the reference period; σ is the Boltzmann constant, α is surface albedo, and clr indicates clear-sky conditions.

3. Results

3.1. *Projected near-surface air temperature changes on the TP in response to transient and stabilized 2.0°C/1.5°C global warming*

The average changes in annual and seasonal mean near-surface air temperature in response to transient and stabilized 2.0°C/1.5°C global warming are displayed in Fig. 3. Changes in annual mean temperature on the TP in a 1.5°C (2.0°C) warmer world relative to the reference period (1961–90) are 1.75°C (2.50)°C, 1.80°C (2.53)°C, and 1.57°C (2.33)°C, derived from RCP8.5, RCP4.5, and low-warming simulations, respectively. The above results indicate that the warming rate on the TP is much faster than global average warming, which is consistent with the findings of You et al. 2020a. The magnitudes of warming are more pronounced in the cold season (Oct.–Mar.) than in the warm season (Apr.–Sep.), also consistent with previous studies (Wu et al., 2019; Fu et al., 2021). The cold season mean

temperature increases are 12%–17% (mean 14%) higher than the increases in annual mean temperature for a 1.5°C (2.0°C) warmer world. Similar to the above results, the increase in temperature associated with the additional 0.5°C of global warming is greater in the cold season than in the warm season (Fig. 2).

Temperature increases in the transient warming world are higher than those in the stabilized world at the same global warming level. For example, projected changes of annual mean temperature in futures that are 2.0°C/1.5°C warmer relative to the reference period are ~0.2°C higher in transient simulations than stabilized simulations. A similar phenomenon can be observed in the changes of seasonal mean temperature (0.17°C–0.23°C) under the corresponding scenarios.

The spatial distributions of annual and seasonal mean temperature changes in transient and stabilized warmer futures are displayed in Fig. 4 (annual) and Fig. S1 (seasonal) in the electronic supplementary materials (ESM). Temperature changes in 2.0°C or 1.5°C scenarios relative to the reference period are broadly similar in terms of their spatial pattern; therefore, we only display the results of the 1.5°C scenarios. The regions with the most pronounced increase in annual mean near-surface air temperature in the 21st century tend to be centered along the southwestern edge of the TP. The spatial pattern of changes in seasonal temperatures is generally similar to those in the annual mean, although slight differences are observable. The magnitude and spatial pattern of temperature changes under the two transient scenarios (RCP8.5 and RCP4.5) are quite similar; hence we can consider the average of these as the results of transient simulations and further compare them with those of the stabilized simulations (right-hand column). There is no marked difference between the spatial patterns of temperature changes on the TP in response to transient versus stabilized warming, even though the magnitudes vary. The spa-

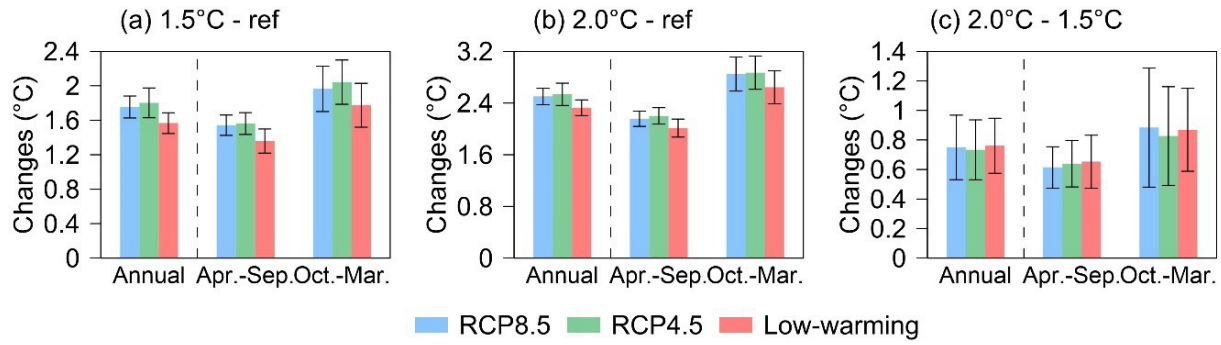

Fig. 3. Regionally-averaged near-surface temperature changes on the TP. The reference period is 1961–90. (a) 1.5°C scenario versus the reference period; (b) 2.0°C scenario versus the reference period; (c) 2.0°C scenario versus 1.5°C scenario. All changes are statistically significant according to the Wilcoxon Rank Sum test ($\alpha = 0.05$). Error bars indicate the standard deviation across ensemble members.

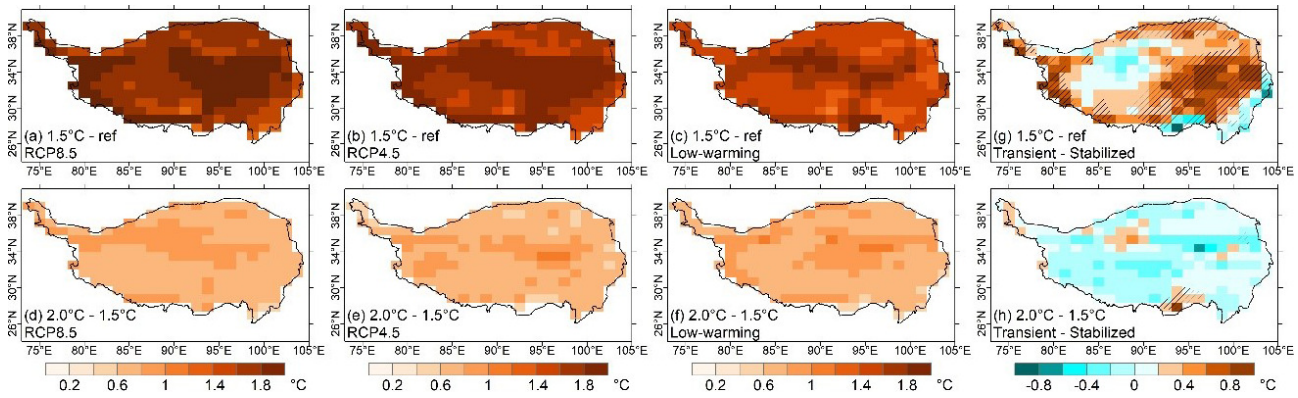

Fig. 4. Spatial pattern of annual mean near-surface air temperature changes on the TP. (a–c) 1.5°C scenario versus the reference period; (d–f) 2.0°C scenario versus the 1.5°C scenario. Panels (a) and (d) are transient responses derived from the RCP8.5 scenario. Panels (b) and (e) are transient responses derived from RCP4.5 simulation; Panels (c) and (f) are stabilized responses derived from the low-warming simulation. The white mask in (a–f) is applied for areas where changes are not statistically significant according to the Wilcoxon Rank Sum test ($\alpha = 0.05$). The differences between the results derived from the transient simulations and stabilized simulations are displayed in (g–h): (g) 1.5°C scenario versus the reference period; (h) 2.0°C scenario versus the 1.5°C scenario. "Transient" refers to the averaged results from the RCP8.5 and RCP4.5 simulations, whereas "Stabilized" refers to the low-warming simulations. Hatching in (g–h) is applied for areas where differences are statistically significant according to Wilcoxon Rank Sum test ($\alpha = 0.05$).

tial distributions of temperature differences associated with an additional 0.5°C global warming show roughly similar patterns to the differences between the 1.5°C warmer future and the reference period, while the magnitudes vary (Figs. 4 and S1 in the ESM).

It can be speculated that the spatial heterogeneity of temperature variation is likely correlated with elevation. To further explore this, Figure 5 displays the annual and seasonal mean near-surface temperature changes in future scenarios for elevation bands of 2500–3000, 3000–3500, 3500–4000, 4000–4500, 4500–5000, and 5000–5500 m. Annual and winter temperature changes exhibit clearer EDW than in the summer. The increase in mean near-surface temperature tends to become greater as elevation increases, and, in general, the areas around 4500–5500 m exhibit the most pronounced warming.

By examining the contrast in EDW between transient and stabilized warming scenarios, we see that in the transient simulations, warming increases strongly up to 4500 m, but above this level, there is an insignificant correlation with elevation. In stabilized scenarios, the warming continues to increase up to 5500 m. On average, more rapid warming is observed at elevations over 4000 m in transient simulations than stabilized simulations. The difference in warming between transient and stabilized scenarios of the same global warming target (right-hand column) shows a complex elevational profile, with the peak difference observed between 4000–4500 m.

Although previous studies have reported TP warming magnitudes in 2.0°C and 1.5°C warmer futures, those results are mainly derived from transient RCP simulations (Wu et al., 2019; You et al., 2019), which do not meet the long-term targets of the Paris Agreement. Our results show considerable differences in temperature increases between future transient and stabilized scenarios for the same global warming target, which previous studies have not examined. Our results also confirm the existence of positive EDW on the TP in most future warming scenarios.

3.2. *Analysis of factors influencing temperature change on the TP*

We further investigate the physical mechanisms which may account for temperature changes on the TP in the context of global warming based on the energy balance equation (Lu and Cai, 2009) described in section 2. Although, strictly speaking, this method targets surface temperature (rather than near-surface air temperature), the relative magnitude of the terms on the right side of Eq. 1 can be interpreted as the relative importance (contribution) of each factor to TP warming. We also verify that changes in surface temperature (Ts) and near-surface air temperature (Tas) are broadly similar (Figs. 6–7). Changes in future scenarios compared with the reference period, as well as the differences between various future scenarios, are similar for both Ts and Tas. In the following analysis, we compare future scen-

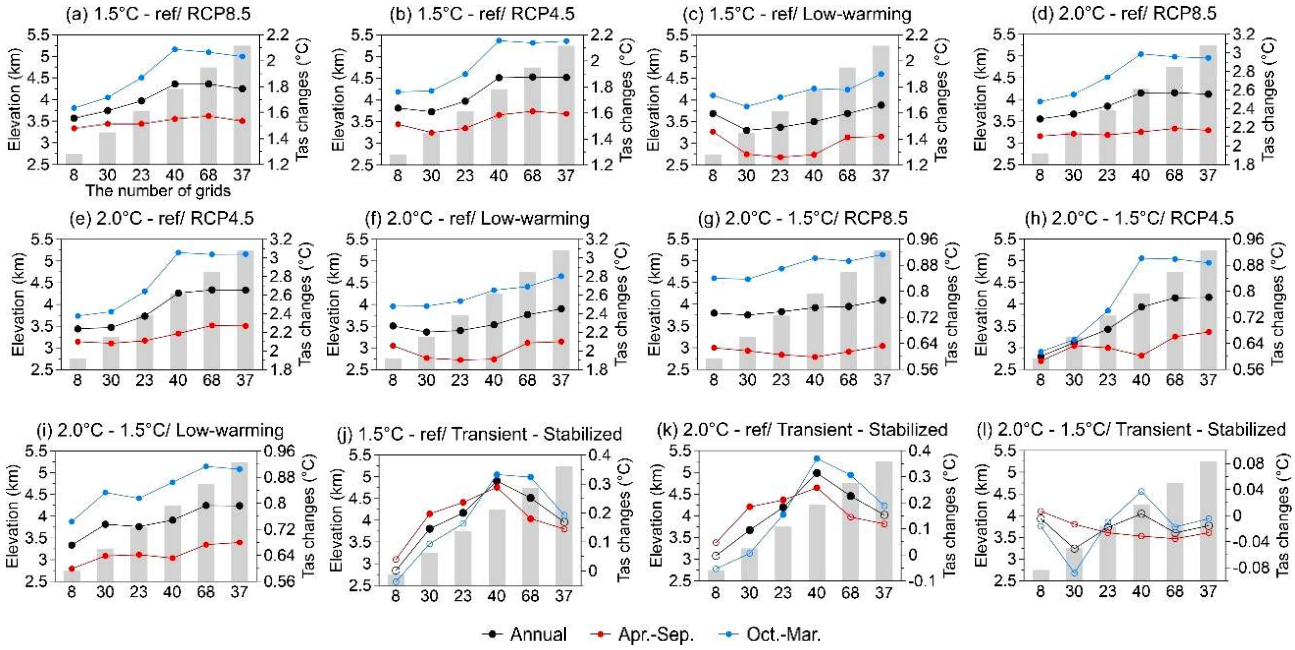

Fig. 5. Projected near-surface air temperature changes for different elevation ranges under the different transient and stabilized scenarios. The number of model grid cells within each elevation band is displayed below the *x*-axis. (a–d): 1.5°C scenario versus the reference period. (e–h): 2.0°C scenario versus the reference period. (i–l): 2.0°C scenario versus 1.5°C scenario. Panels (a), (e), and (i) are transient responses derived from the RCP8.5 scenario; Panels (b), (f), and (j) are transient responses derived from the RCP4.5 simulation; Panels (c), (g), and (k) are stabilized responses derived from low-warming simulation. In panels (d), (h), and (l), "Transient" refers to the averaged results from the RCP8.5 and RCP4.5 simulations, whereas "Stabilized" refers to the low-warming simulations. Results of annual (black) and seasonal changes (winter: blue and summer: red) are displayed in different colors (also see legend in (a)). Solid dots indicate that the changes are statistically significant according to the Wilcoxon Rank Sum test ($\alpha = 0.05$).

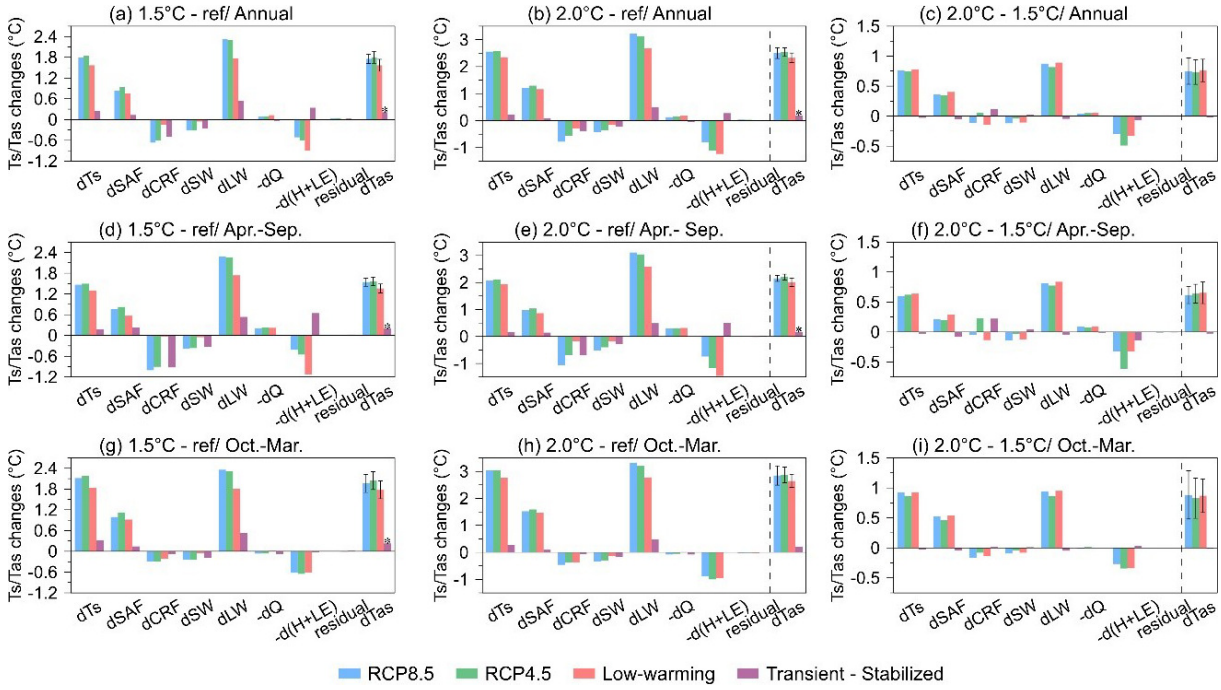

Fig. 6. Analysis of factors influencing temperature changes on the TP under the different transient and stabilized scenarios. Changes in surface temperature (dTs - left) and the seven decomposition terms given in Eq. 1, as well as changes in near-surface air temperature (dTas - right) are displayed. Panels (a), (d), and (g) indicate the 1.5°C scenario versus the reference period; Panels (b), (e), and (h) indicate the 2.0°C scenario versus the reference period; Panels (c), (f), and (i) indicate 2.0°C scenario versus 1.5°C scenario. (a–c) indicate annual mean changes, (d–f) indicate the summer half-year mean changes, and (g–i) indicate the winter half-year mean changes. Blue and green bars indicate the transient response derived from the RCP8.5 and RCP4.5 simulations, respectively. Red bars indicate the stabilized response derived from low-warming simulations. Purple bars indicate the difference between the transient and stabilized response, among them, "Transient" refers to the average of the results from RCP8.5 and RCP4.5 simulations, whereas "Stabilized" refers to the low-warming simulations. Error bars for dTas indicate the standard deviation across ensemble members. Asterisks on the purple bars for dTas indicate differences between results from transient and stabilized simulations are statistically significant according to the Wilcoxon Rank Sum test ($\alpha = 0.05$).

arios to the reference period.

We first examine the TP as a whole (Fig. 6). The projected TP warming is dominated by enhanced downward clear-sky LW, which is related to the net effect of changes in atmospheric CO_2 concentration, water vapor, and air temperature (Lu and Cai, 2009; Ji et al., 2020). Surface albedo feedback (SAF) is the second-largest contributor to the TP warming with observable seasonal differences (greater contribution in the cold season when changes in snow cover presumably play an important role). Cloud radiative feedback (CRF) exerts a moderately negative effect on TP warming with significant seasonal differences (it is strongest in the warm season). Decreased downward clear-sky SW and changes in thermal storage make minor contributions towards temperature changes on the TP. Changes in surface sensible and latent heat fluxes contribute to adjusting the ground-air temperature difference (Ts–Tas).

The differential response of TP warming to transient, as opposed to stabilized 2.0°C/1.5°C global warming, is of concern. The greater increase in surface temperature under transient scenarios relative to that under stabilized scenarios can be interpreted as a result of enhanced downward clear-sky LW, weakened surface sensible and latent heat fluxes, and increased SAF, while negative effects of CRF and weaker downward clear-sky SW partly cancel the positive effects above. When global warming reaches the given threshold (i.e., 1.5°C and 2.0°C), the atmospheric CO_2 concentration and associated radiative forcing are higher in transient simulations than in stabilized simulations (Table 1), and the resulting differences in downward clear-sky LW become clearly evident (Fig. 6). However, significant differences in CRF are also noticeable between the transient and stabilized scenarios. Further investigation is needed to investigate the extent to which this could be related to distinct differences in atmospheric circulation between the two scenarios (Ji et al., 2020).

In addition, we attempt to reveal the mechanisms responsible for EDW across the TP from the perspective of surface energy balance. Annual and seasonal mean temperature changes in separate elevation bands are displayed in Fig. 7 (annual) and Figs. S2–S3 (seasonal), respectively. The warming effect induced by enhanced downward clear-sky LW radiation dominates the temperature increase in all elevation bands, and the elevation dependence of this effect is unre-

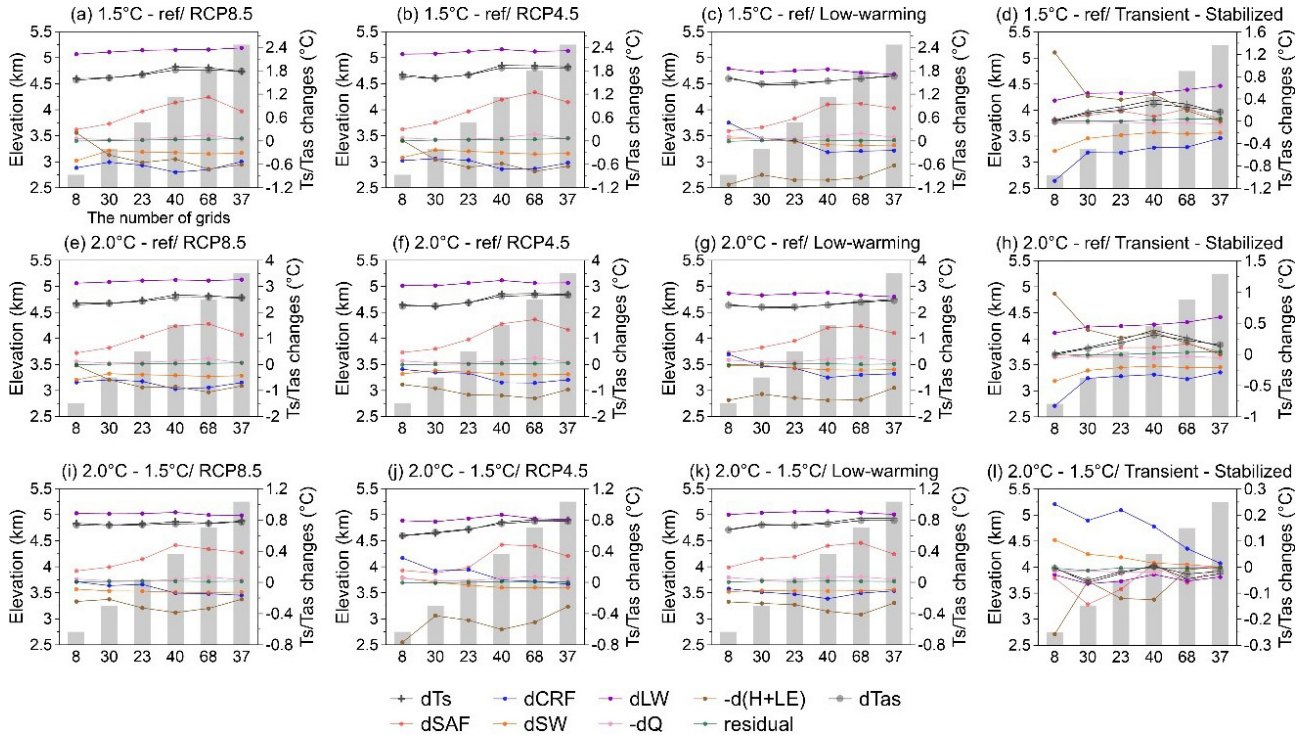

Fig. 7. Elevation profiles of factors influencing annual temperature changes on the TP. Changes in surface temperature (dTs) and the seven decomposition terms given in Eq. 1, as well as changes in near-surface air temperature (dTas) are displayed (see legend). (a–d) 1.5°C scenario versus the reference period; (e–h) 2.0°C scenario versus the reference period; (i–l) 2.0°C scenario versus the 1.5°C scenario. Panels (a), (e), and (i) are the transient responses derived from RCP8.5 scenario. Panels (b), (f), and (j) are the transient responses derived from RCP4.5 simulation. Panels (c), (g), and (k) are the stabilized responses derived from the low-warming simulation. Panels (d), (h), and (l) are the differences between the transient and stabilized responses, among them, "Transient" refers to the averaged results from RCP8.5 and RCP4.5 simulations, whereas "Stabilized" refers to the low-warming simulations.

markable. On the other hand, the SAF exhibits the most significant elevation dependence of all terms on the right side of Eq. 1, with a maximum effect between 4000–5000 m. In addition, the elevation dependence of CRF in the summer half-year is relatively obvious, decreasing at higher elevations. The elevation dependence of the remaining terms is less pronounced. Noting the strikingly similar profiles between EDW and SAF-induced temperature changes, it can be inferred that even though TP warming as a whole is dominated by enhanced downward clear-sky LW, the EDW component is broadly dominated by the heterogeneity of SAF at different elevations, presumably related to elevational contrasts in future snow cover. Other factors also contribute to some extent to EDW on the TP. There is no clear single factor that correlates with the elevation-dependent difference in temperature changes for transient vs. stabilized scenarios at the same global warming level (the right-hand column in Figs. 7 and S2–S3 in the ESM).

4. Discussion and conclusions

4.1. *Discussion*

Our results reveal the TP warming response to the global temperature targets set by the Paris Agreement and demonstrate important differences between stabilized and transient scenarios with the same warming target. Warming is projected to be ~0.2°C higher in transient scenarios than in stabilized scenarios, consistent with similar studies (Wei et al., 2019). We further demonstrate that EDW on the TP exists in both 2.0°C and 1.5°C warmer futures, which complements the findings of You et al. (2019). These results further emphasize the importance of accounting for the differences between transient and stabilized scenarios in projection studies of climate change impact (Zhang and Zhou, 2021). Even at the same global warming level, the differences between fast-warming ("transient") and stable climates are locally observable (e.g., on the Tibetan plateau); hence these differences need to be considered in adapting to future climate change.

This study also proposes an energy budget analysis for interpreting future EDW on the TP. Previous studies have already shown that the warming rate on the TP generally increases with altitude up to around 5000 m, but that it may not increase further at higher altitudes (Qin et al., 2009; Gao et al., 2018; Guo et al., 2019; Zhang et al., 2022). The presence of EDW on the TP has been attributed to several factors, summarized by You et al. (2020b). Among them, snow cover change is considered to be one of the most important, outlined by the SAF mechanism (Ghatak et al., 2014; Guo et al., 2021; Shen et al., 2021). We substantiate the important role of the SAF mechanism in shaping EDW

from the perspective of an energy budget analysis. The elevations around 4000–5000 m exhibit the most pronounced warming trends, and this elevation range is where annual mean temperatures are around 0°C, that is, the location of the snow line. Snow cover which surrounds the mean snow line position is relatively shallow, and the snow-albedo feedback is large where regular snow cover disappears (Brown and Mote, 2009; You et al., 2010, 2019). In the higher altitude regions (>5000 m) on the TP, snow cover is present all year round due to low temperatures. The effect of snow-albedo feedback is thus relatively small (Gao et al., 2018; Zhang et al., 2022), at least in the 21st-century simulations. In addition, future warming on the TP is also affected by cloud, aerosol, land-use change, ozone, vegetation, and other factors (You et al., 2020b). Although a complete physical attribution of the EDW on the TP requires further surface energy budget analysis, the approach contributes a new holistic explanation of future changes.

4.2. *Conclusions*

This study quantifies the TP warming response to both transient and stabilized 2.0°C/1.5°C global warming based on a suite of simulations using the CESM model and further explores the underlying mechanisms from the perspective of a surface energy budget analysis. The main findings are summarized as follows:

(1) The projected warming rate on the TP is much faster than mean global warming under 1.5°C and 2.0°C global warming scenarios. Greater warming occurs in the cold season, averaging ~14% above the annual mean level. The warming response of the plateau is ~0.2°C higher under transient scenarios than under stabilized scenarios for the same overall global warming. The TP warming relative to the reference period is strongly correlated to an enhancement of downward clear-sky longwave radiation. At the same time, the differences between transient and stabilized scenarios are primarily caused by the combined effects of differential downward longwave radiation, cloud radiative forcing, and surface sensible and latent heat fluxes.

(2) TP warming relative to the reference period exhibits strong EDW in both 2.0°C and 1.5°C warmer futures, especially in winter. The difference in TP warming between transient and stabilized scenarios of the same global warming target shows a relatively weak EDW signal. The most pronounced warming trends occur around 4000–5000 m. Surface albedo feedback associated with changes in the cryosphere and the surface snow cover shapes the profile of EDW relative to the reference period.

Acknowledgements. This study is supported by the National Natural Science Foundation of China (Grant Nos. 41971072, 41771069). We are grateful to the reviewers for their constructive comments and thoughtful suggestions.

Electronic supplementary material: Supplementary material is available in the online version of this article at https://doi.org/10.1007/s00376-022-1299-8.

REFERENCES

Brown, R. D., and P. W. Mote, 2009: The response of northern hemisphere snow cover to a changing climate. *J. Climate*, **22**, 2124–2145, https://doi.org/10.1175/2008JCLI2665.1.

Cai, D. L., Q. L. You, K. Fraedrich, and Y. N. Guan, 2017: Spatiotemporal temperature variability over the Tibetan Plateau: Altitudinal dependence associated with the Global warming hiatus. *J. Climate*, **30**, 969–984, https://doi.org/10.1175/JCLI-D-16-0343.1.

Duan, A. M., G. X. Wu, Y. M. Liu, Y. M. Ma, and P. Zhao, 2012: Weather and climate effects of the Tibetan Plateau. *Adv. Atmos. Sci.*, **29**(5), 978–992, https://doi.org/10.1007/s00376-012-1220-y.

Fu, Y.-H., R.-Y. Lu, and D. Guo, 2018: Changes in surface air temperature over China under the 1.5°C and 2.0°C global warming targets. *Advances in Climate Change Research*, **9**, 112–119, https://doi.org/10.1016/j.accre.2017.12.001.

Fu, Y.-H., X.-J. Gao, Y.-M. Zhu, and D. Guo, 2021: Climate change projection over the Tibetan Plateau based on a set of RCM simulations. *Advances in Climate Change Research*, **12**, 313–321, https://doi.org/10.1016/j.accre.2021.01.004.

Gao, Y. H., F. Chen, D. P. Lettenmaier, J. W. Xu, L. H. Xiao, and X. Li, 2018: Does elevation-dependent warming hold true above 5000 m elevation? Lessons from the Tibetan Plateau *npj Climate and Atmospheric Science*, **1**, 19, https://doi.org/10.1038/s41612-018-0030-z.

Ghatak, D., E. Sinsky, and J. Miller, 2014: Role of snow-albedo feedback in higher elevation warming over the Himalayas, Tibetan Plateau and Central Asia. *Environmental Research Letters*, **9**, 114008, https://doi.org/10.1088/1748-9326/9/11/114008.

Guo, D. L., J. Q. Sun, K. Yang, N. Pepin, and Y. M. Xu, 2019: Revisiting recent elevation-dependent warming on the Tibetan Plateau using satellite-based data sets. *J. Geophys. Res.*, **124**, 8511–8521, https://doi.org/10.1029/2019JD030666.

Guo, D. L., N. Pepin, K. Yang, J. Q. Sun, and D. Li, 2021: Local changes in snow depth dominate the evolving pattern of elevation-dependent warming on the Tibetan Plateau. *Science Bulletin*, **66**, 1146–1150, https://doi.org/10.1016/j.scib.2021.02.013.

Ji, P., X. Yuan, and D. Li, 2020: Atmospheric radiative processes accelerate ground surface warming over the southeastern Tibetan Plateau during 1998–2013. *J. Climate*, **33**, 1881–1895, https://doi.org/10.1175/JCLI-D-19-0410.1.

Kang, S. C., Y. W. Xu, Q. L. You, W.-A. Flügel, N. Pepin, and T. D. Yao, 2010: Review of climate and cryospheric change in the Tibetan Plateau. *Environmental Research Letters*, **5**, 015101, https://doi.org/10.1088/1748-9326/5/1/015101.

Kay, J. E., and Coauthors, 2015: The community earth system model (CESM) large ensemble project: A community resource for studying climate change in the presence of internal climate variability. *Bull. Amer. Meteor. Soc.*, **96**, 1333–1349, https://doi.org/10.1175/BAMS-D-13-00255.1.

Li, B. F., Y. N. Chen, and X. Shi, 2020: Does elevation dependent warming exist in high mountain Asia. *Environmental Research Letters*, **15**, 024012, https://doi.org/10.1088/1748-9326/ab6d7f.

Lu, J. H., and M. Cai, 2009: Seasonality of polar surface warming amplification in climate simulations. *Geophys. Res. Lett.*, **36**, L16704, https://doi.org/10.1029/2009GL040133.

Lun, Y. R., L. Liu, L. Cheng, X. P. Li, H. Li, and Z. X. Xu, 2021: Assessment of GCMs simulation performance for precipitation and temperature from CMIP5 to CMIP6 over the Tibetan Plateau. *International Journal of Climatology*, **41**, 3994–4018, https://doi.org/10.1002/joc.7055.

Niu, X. R., J. P. Tang, D. L. Chen, S. Y. Wang, and T. H. Ou, 2021: Elevation-dependent warming over the Tibetan Plateau from an ensemble of CORDEX-EA regional climate simulations. *J. Geophys. Res.*, **126**, e2020JD033997, https://doi.org/10.1029/2020JD033997.

Qin, J., K. Yang, S. L. Liang, and X. F. Guo, 2009: The altitudinal dependence of recent rapid warming over the Tibetan Plateau. *Climatic Change*, **97**, 321–327, https://doi.org/10.1007/s10584-009-9733-9.

Sanderson, B. M., and Coauthors, 2017: Community climate simulations to assess avoided impacts in 1.5°C and 2°C futures. *Earth System Dynamics*, **8**, 827–847, https://doi.org/10.5194/esd-8-827-2017.

Sanderson, B. M., K. W. Oleson, W. G. Strand, F. Lehner, and B. C. O'Neill, 2018: A new ensemble of GCM simulations to assess avoided impacts in a climate mitigation scenario. *Climatic Change*, **146**, 303–318, https://doi.org/10.1007/s10584-015-1567-z.

Shen, L. C., Y. Q. Zhang, S. Ullah, N. Pepin, and Q. R. Ma, 2021: Changes in snow depth under elevation-dependent warming over the Tibetan Plateau. *Atmospheric Science Letters*, **22**, e1041, https://doi.org/10.1002/asl.1041.

Shi, C., Z.-H. Jiang, L.-H. Zhu, X. B. Zhang, Y.-Y. Yao, and L. Li, 2020: Risks of temperature extremes over China under 1.5°C and 2°C global warming. *Advances in Climate Change Research*, **11**, 172–184, https://doi.org/10.1016/j.accre.2020.09.006.

Tebaldi, C., and Coauthors, 2021: Climate model projections from the Scenario Model Intercomparison Project (ScenarioMIP) of CMIP6. *Earth System Dynamics*, **12**, 253–293, https://doi.org/10.5194/esd-12-253-2021.

UNFCCC, 2015: Adoption of the Paris Agreement. Proposal by the President. Report No. Proposal by the President. FCCC/CP/2015/L.9/Rev.1. [Available online from https://unfccc.int/sites/default/files/resource/docs/2015/cop21/eng/l09r01.pdf].

Wang, T., Y. T. Zhao, C. Y. Xu, P. Ciais, D. Liu, H. Yang, S. L. Piao, and T. D. Yao, 2021: Atmospheric dynamic constraints on Tibetan Plateau freshwater under Paris climate targets. *Nature Climate Change*, **11**, 219–225, https://doi.org/10.1038/s41558-020-00974-8.

Wei, Y., H. P. Yu, J. P. Huang, T. J. Zhou, M. Zhang, and Y. Ren, 2019: Drylands climate response to transient and stabilized 2°C and 1.5°C global warming targets. *Climate Dyn.*, **53**, 2375–2389, https://doi.org/10.1007/s00382-019-04860-8.

Wu, F. Y., Q. L. You, W. X. Xie, and L. Zhang, 2019: Temperature change on the Tibetan Plateau under the global warming of 1.5°C and 2°C. *Climate Change Research*, **15**(2), 130–139, https://doi.org/10.12006/j.issn.1673-1719.2018.175. (in Chinese with English abstract)

Yao, T. D., and Coauthors, 2012: Third pole environment (TPE). *Environmental Development*, **3**, 52–64, https://doi.org/10.1016/j.envdev.2012.04.002.

Yao, T. D., and Coauthors, 2019: Recent third pole's rapid warming accompanies cryospheric melt and water cycle intensification and interactions between monsoon and environment: Multidisciplinary approach with observations, modeling, and analysis. *Bull. Amer. Meteor. Soc.*, **100**, 423–444, https://doi.org/10.1175/BAMS-D-17-0057.1.

You, Q. L., S. C. Kang, N. Pepin, W.-A. Flügel, Y. P. Yan, H. Behrawan, and J. Huang, 2010: Relationship between temperature trend magnitude, elevation and mean temperature in the Tibetan Plateau from homogenized surface stations and reanalysis data. *Global and Planetary Change*, **71**, 124–133, https://doi.org/10.1016/j.gloplacha.2010.01.020.

You, Q. L., J. Z. Min, and S. C. Kang, 2016: Rapid warming in the Tibetan Plateau from observations and CMIP5 models in recent decades. *International Journal of Climatology*, **36**, 2660–2670, https://doi.org/10.1002/joc.4520.

You, Q. L., Y. Q. Zhang, X. Y. Xie, and F. Y. Wu, 2019: Robust elevation dependency warming over the Tibetan Plateau under global warming of 1.5°C and 2°C. *Climate Dyn.*, **53**, 2047–2060, https://doi.org/10.1007/s00382-019-04775-4.

You, Q. L., F. Y. Wu, L. C. Shen, N. Pepin, Z. H. Jiang, and S. C. Kang, 2020a: Tibetan Plateau amplification of climate extremes under global warming of 1.5°C, 2°C and 3°C. *Global and Planetary Change*, **192**, 103261, https://doi.org/10.1016/j.gloplacha.2020.103261.

You, Q. L., and Coauthors, 2020b: Elevation dependent warming over the Tibetan Plateau: Patterns, mechanisms and perspectives. *Earth-Science Reviews*, **210**, 103349, https://doi.org/10.1016/j.earscirev.2020.103349.

You, Q. L., and Coauthors, 2021: Warming amplification over the Arctic Pole and Third Pole: Trends, mechanisms and consequences. *Earth-Science Reviews*, **217**, 103625, https://doi.org/10.1016/j.earscirev.2021.103625.

Zhang, H. B., W. W. Immerzeel, F. Zhang, R. J. De Kok, D. L. Chen, and W. Yan, 2022: Snow cover persistence reverses the altitudinal patterns of warming above and below 5000 m on the Tibetan Plateau. *Science of the Total Environment*, **803**, 149889, https://doi.org/10.1016/j.scitotenv.2021.149889.

Zhang, J. T., and F. Wang, 2019: Changes in the risk of extreme climate events over East Asia at different global warming levels. *Water*, **11**, 2535, https://doi.org/10.3390/w11122535.

Zhang, W. X., and T. J. Zhou, 2021: The effect of modeling strategies on assessments of differential warming impacts of 0.5°C. *Earth's Future*, **9**, e2020EF001640, https://doi.org/10.1029/2020EF001640.

Zhang, Z. X., J. Chang, C.-Y. Xu, Y. Zhou, Y. H. Wu, X. Chen, S. S. Jiang, and Z. Duan, 2018: The response of lake area and vegetation cover variations to climate change over the Qinghai-Tibetan Plateau during the past 30 years. *Science of the Total Environment*, **635**, 443–451, https://doi.org/10.1016/j.scitotenv.2018.04.113.